Eur. Phys. J. D **30**, 225–233 (2004)
DOI: 10.1140/epjd/e2004-00081-7

THE EUROPEAN PHYSICAL JOURNAL D

On the coupling of electron energy distribution function and excited state distributions in pulsed microwave H_2 plasmas

G. Lombardi[1], X. Duten[1], K. Hassouni[1], M. Capitelli[2,a], and A. Gicquel[1]

[1] LIMHP, CNRS-UPR1311, Université de Paris-Nord, 93430 Villetaneuse, France
[2] IMIP-CNR and Dept. Chemistry University of Bari, Via Orabona 4, 70100 Bari, Italy

Received 15 January 2004
Published online 29 June 2004 –

Abstract. Time evolution of vibrationally and electronically excited states and their coupling with the electron energy distribution function (EEDF) were calculated for microwave pulsed discharges. Different situations have been considered by changing the period and the duty cycle, and considering different pressure values.The main result of this study was to evidence the change in the non-equilibrium character and dynamics of the different distributions depending on the pressure and the pulse period. In particular EEDF strongly deviating from the Maxwell behaviour appear as a consequence of inelastic and superelastic collisions at relatively high pressure and long period. Also, strong oscillation appears on the tail of the H_2 vibrational distribution at high pressure discharge conditions. At low pressure, the effect of superelastic and inelastic collisions appears to be less significant and most of the plasma characteristics may be deduced from a time averaged electron energy distribution function.

PACS. 52.25.Dg Plasma kinetic equations – 52.20.Hv Atomic, molecular, ion, and heavy-particle collisions – 52.27.Cm Multicomponent and negative-ion plasmas

1 Introduction

Large interest is presently devoted to the study of pulsed H_2 discharges for many technological applications including plasma assisted diamond deposition [1] and negative ion formation [2]. This interest demands a parallel theoretical study to follow the time history of the different plasma characteristics during and in between the microwave pulses. In this context the study of the time-evolution of the non-equilibrium vibrational distributions (VDF) and the electron energy distribution functions (EEDF) in pulsed microwave discharges becomes of prime interest. Previous studies dealt in particular with the coupling of EEDF, VDF and electronically excited distribution function of molecular and atomic species (EEDFMAS) in the post discharge regime [3,4]. Starting from stationary EEDF and EEDFMAS distribution functions that corresponds to a given discharge conditions we have followed the temporal evolution in the post discharge regime once the electric field sustaining the discharge was switched off. To this end, we made use of a sophisticated kinetic model [5] including: (1) the vibrational kinetics of ground state; (2) a collisional radiative model for electronically excited molecular and atomic hydrogen; (3) a plasma chemistry model for atoms and ions; (4) a Boltzmann equation for the electron energy distribution function. The most significant result of this study was the evidence of many structures that appears in the EEDF as a result of second kind collisions between cold electrons and electronically excited states [4].

The aim of the present study is to extend this kind of calculations to microwave pulsed discharges. In this case we are interested in the time-evolution of EEDF, VDF, EEDFMAS and atom and negative ion densities during several power pulses. We are especially interested in the evolution of the plasma characteristics at the beginning of the power-on (in-pulse) power-off (post-discharge) periods. In the last case we are interested in the relaxation kinetics of the different plasma characteristics, while in the former our aim is to investigate the electron heating dynamics and the excitation kinetics of the different excitation modes. Also of interest are the modulation amplitude of the different plasma characteristics and the resulting *average* plasma. The change in the plasma conditions is investigated as function of the input microwave power, the working pressure, the pulse period and the duty cycle. This last parameter is defined as the ratio of the duration of the power-on phase and the pulse period.

Changing these controlling parameters allows us studying how the interplay between the different non-equilibrium processes can affect the different plasma characteristics.

[a] e-mail: capitelli@area.ba.cnr.it

2 The kinetic model

The kinetic model describing microwave plasmas has been fully described in reference [5]. Basically it includes:

(a) a time dependent Boltzmann equation for the electron energy distribution (EEDF) including the electric field term, elastic, inelastic and superelastic collisions from both vibrationally and electronically excited states;
(b) a non equilibrium vibrational kinetics for describing the vibrational distribution function (VDF) of H_2 molecules ($n = 0{-}14$);
(c) a collisional radiative model describing the population of electronically excited states of both atomic and molecular hydrogen;
(d) a chemistry model for the species H_2^+, H_3^+, H^+ and H^- and electrons;
(e) a quasi-homogeneous plasma transport model for the estimation of species losses at the plasma reactor wall;
(f) a total energy equation that yields the gas temperature.

Time-dependent EEDF is obtained by solving the two-term expansion of the homogeneous Boltzmann equation that may be written as

$$\frac{dn(\varepsilon,t)}{dt} = -\frac{dJ_f}{d\varepsilon} - \frac{dJ_{el}}{d\varepsilon} - \frac{dJ_{e-e}}{d\varepsilon} + In + Sup \quad (1)$$

where $n(\varepsilon,t)de$ is the density of electrons with energy between ε and $\varepsilon + d\varepsilon$ at a time t.

The different terms on the right hand side of equation (1) involves the flux of electrons in the energy space due to the electric field (J_f), to the elastic collisions (J_{el}) and to electron-electron Coulomb collisions (J_{e-e}). It also involves the source terms corresponding to inelastic (In) and superelastic (Sup) collisions. Detailed expressions of the flux and source terms involved in (1) can be found in references [6,7]. Due to the small ionization degrees considered in the different case studies, the electron-electron collision flux term was neglected in the present work.

The integration of the Boltzmann equation requires the knowledge of the microwave electric field amplitude that is a priori unknown. This amplitude, or the corresponding root mean square (rms) value, may be determined from the absorbed microwave power density that is a model parameter. For this purpose the following additional algebraic equation that expresses the dependence between the electric field and the absorbed microwave power density (MWPD) was coupled to the electron Boltzmann and species balance equations [5]:

$$E(t) = \frac{E_{rms}}{\sqrt{2}}\cos(\omega t) = E_0\cos(\omega t) \quad (2)$$

$$E_{rms} = \left(MWPD\frac{m_e}{n_e e^2}\right)^{1/2}\left(\int_\varepsilon \frac{\nu}{\nu^2+\omega^2} f(\varepsilon)d\varepsilon\right)^{1/2} \quad (3)$$

where ω is the angular frequency of the excitation microwave, m_e, e, n_e, ε and $f(\varepsilon)$ are the mass, the charge, the density, the energy and the distribution function of electrons. $\nu(\varepsilon)$ is the electron-heavy particle elastic collision frequency.

The vibrational kinetics includes several electron impact and heavy species — heavy species elementary processes. In particular we considered the pumping of vibrational quanta by electron impact through resonant (4) and indirect (5) processes

$$e + H_2(v) \Rightarrow H_2^- \Rightarrow e + H_2(w) \quad (4)$$

$$e + H_2(v) \Rightarrow e + H_2(B^1\Sigma_u^+, C^1\Pi_u) \Rightarrow e + H_2(v') + h\nu. \quad (5)$$

We also considered their redistribution by vibration-vibration (6) and vibration-H_2 translation (7) or vibration-H translation (8) energy exchange processes:

$$H_2(v) + H_2(w) \Rightarrow H_2(v-1) + H_2(w+1) \quad (6)$$

$$H_2(v) + H_2 \Rightarrow H_2(v-1) + H_2 \quad (7)$$

$$H_2(v) + H \Rightarrow H_2(v-1) + H. \quad (8)$$

The dissociation of hydrogen molecules takes place by processes promoted either by electron impact

$$e + H_2(v) \Rightarrow e + H_2^*\left(a^3\Sigma_g, e^3\Sigma_u^+, c^3\Pi_u, b^3\Sigma_u^+\right) \Rightarrow e + 2H \quad (9)$$

or heavy particle collisions

$$H + H_2(v) \Rightarrow 3H \quad (10)$$

$$H_2 + H_2(v) \Rightarrow H_2 + 2H. \quad (11)$$

Heavy particle dissociation is described by the ladder-climbing model, i.e. a model that considers dissociation as the crossing through a pseudo-level located just above the last ($n = 14$) bounded level of the molecule as well as direct processes involving multiquantum transitions [5].

The collisional-radiative model for excited atomic species includes the usual processes induced by electrons (excitation-deexcitation, ionization-recombination). We also considered electronic energy transfer and ionization processes induced by collisions between hydrogen atoms. Several radiative processes were also considered and the plasma was assumed to be optically thick for Lyman lines. The following ionization processes through the reactive quenching of $H(n > 1)$ was considered:

$$H(n) + H_2 = H_3^+ + e. \quad (12)$$

Similar processes are considered for the electronically excited states of the molecule.

The chemistry model for the production of positive and negative ions includes a large number of elementary processes. The most important are:

$$e + H_2(v) \Rightarrow e + H_2^*(X^2\Sigma_g^+, X^2\Sigma_u^+) \Rightarrow e + H^+ + H(1s) \quad (13)$$

$$e + H_2(v) = e + H_2^+ + e \quad (14)$$

$$e + H(n) = e + H^+ + e \quad (15)$$

$$e + H_2(v) = H + H^-. \quad (16)$$

Ion chemistry is also included and takes into account ion conversion, mutual neutralization end dissociative recombination processes. This enables to describe the formation of H_3^+ and negative ions (see Ref. [5] for details).

The quasi-homogeneous model used to estimate the species losses at the substrate surface assumes that the plasma is made of two regions: a uniform bulk and a thin boundary layer where all the species densities vary linearly. Under this assumption, the loss rates are function of the recombination-deexcitation probabilities, the substrate temperature (300 K), the ratio of the wall and substrate surface to the plasma volume.

3 Results

The set of electron Boltzmann, species balance and total energy equations were timeintegrated for square microwave pulses with a constant input power during the in-pulse phase. The plasma parameters for these conditions are:

(1) 10 W power, $p = 1$ torr, $T_{cycle} = 30$ μs, duty cycle 30%;
(2) 10 W power, $p = 1$ torr, $T_{cycle} = 3$ μs, duty cycle 30%;
(3) 10 W power, $p = 10$ mtorr, $T_{cycle} = 3$ μs, duty cycle 30%.

It is worthy to emphasize that a small residual power of about 10^{-2} W (three order of magnitude smaller than the in-pulse power) is coupled to the gas during the out-pulse phase.

First, we discuss a simulation that corresponds to a square pulse with a power amplitude of 10 W, a period T of 30 μs and a duty cycle of 30%. The discharge pressure is 1 torr.

Before examining the results we want to remind that typical relaxation times at 1 torr (300 K) for the different energy zones of EEDF, estimated on the basis of the numerical results reported in reference [8], are of the order of 1 μs for elastic collisions, 3 μs rotational processes and 10 ns for inelastic processes. The characteristic times are therefore less than the considered period, implying a quasistationary behaviour of EEDF and related quantities.

Figure 1 reports the time-evolution of electron average energy for three consecutive pulses starting at a time-value of 100 μs and ending at 200 μs. At the beginning of the first pulse the electron average energy abruptly increases reaching a maximum of about 5.3 eV soon after the start up of the electric field. It then decreases down to about 2 eV, following the variation of the electric field amplitude. As matter of fact, since the power is kept constant during the power on fraction of the cycle, the ionization that takes place during the pulse leads to the increase of the electron density, which leads to the decrease of the electric field and therefore the electron density (see Eq. (3)).

After the end of the power-on fraction of the cycle, the average energy decreases to a very low value that corresponds to an imposed residual electric field. The situation

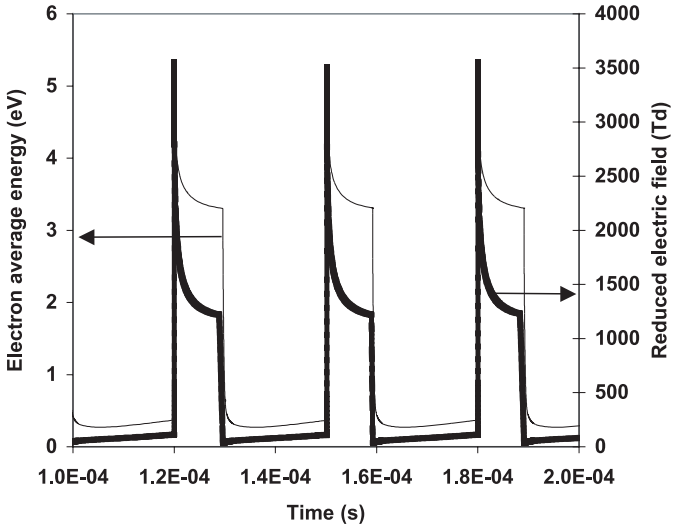

Fig. 1. Time-evolution of the electron average energy and of the reduced electric field in microwave pulsed H_2 discharges ($P = 1$ torr, $MWP_{inp} = 10$ W, $T_{cycle} = 30$ μs, $Duty = 30\%$).

is then perfectly reproducible during the following two periods thus meaning that in the post discharge regime the excited molecules and atoms are not able to affect the average electron energy. Note also that the average energy follows the trend of electric field in a quasistationary way, this means that for the reported conditions the time to reach quasistationary conditions are much shorter than the cycle times as previously pointed out.

Figure 2 reports the evolution of the electron energy distribution (EEDF) during the whole cycle. The EEDF's are reported as a function of the electron energy for different values of the parameter $t' = t/T_{cycle}$. Values of $t' < 0.3$ correspond to power-on fraction of the cycle, while for $t' > 0.3$ we are in the quasi-post-discharge regime with only the residual power coupled to the plasma. The electron energy distribution follows the field, as does the average electron energy, from $t' = 5 \times 10^{-4}$ to $t' = 0.3$, while the plots for $t' > 0.3$ represent the decay of EEDF in the post discharge conditions. We see a quasi-instantaneous electron heating between 5×10^{-4} s and 5×10^{-3} s, followed by a small decrease of EEDF till $t' = 0.3$ due to the decrease of electric field which is, as discussed above, due to the increase of the electron density. The quasistationary plateaus in EEDF obtained between $t' = 0.4$ and $t' = 0.5$ are due to the coupling of EEDF with the electronically excited states through the second kind collisions. This point can be better understood by inspection of the time dependences of the electronically excited state concentrations that are represented in Figure 3 during one pulse-period. Electronically excited molecular species rapidly grow during the duty cycle and are rapidly consumed at the end of the pulse (see Fig. 3). The corresponding molar fractions can reach values as high as 10^{-8} for selected molecular states. These values corresponds to density of about $10^8 - 10^9$ cm^{-3} and are not sufficient to affect EEDF through superelastic collisions during the duty cycle.

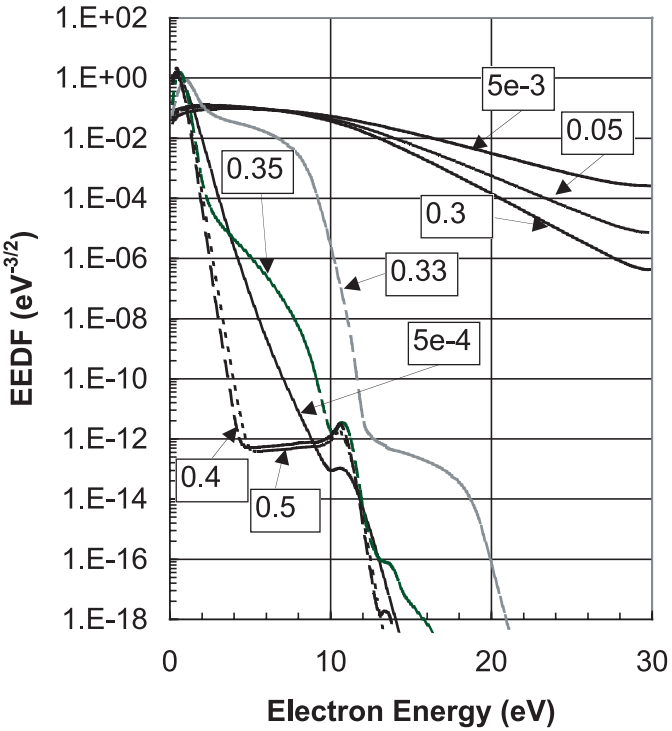

Fig. 2. Electron energy distributions functions versus energy for different phase-values $t' = t/T_{cycle}$ in microwave pulsed H_2 discharges ($P = 1$ torr, $MWP_{inp} = 10$ W, $T_{cycle} = 30$ μs, $Duty = 30\%$).

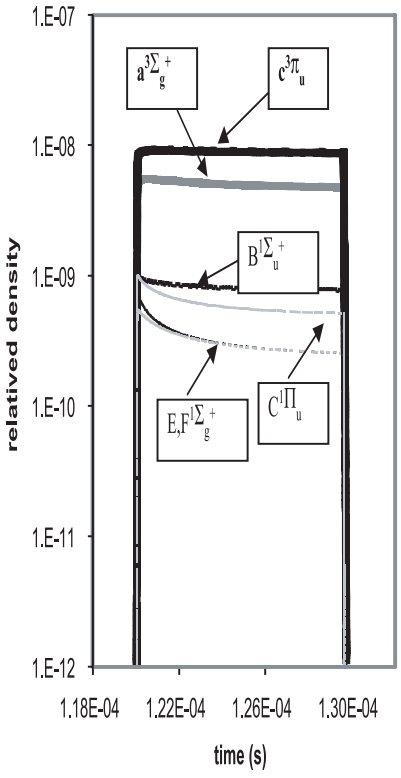

Fig. 3. Time evolution of selected molecular H_2 excited states during one pulse period ($P = 1$ torr, $MWP_{inp} = 10$ W, $T_{cycle} = 30$ μs, $Duty = 30\%$).

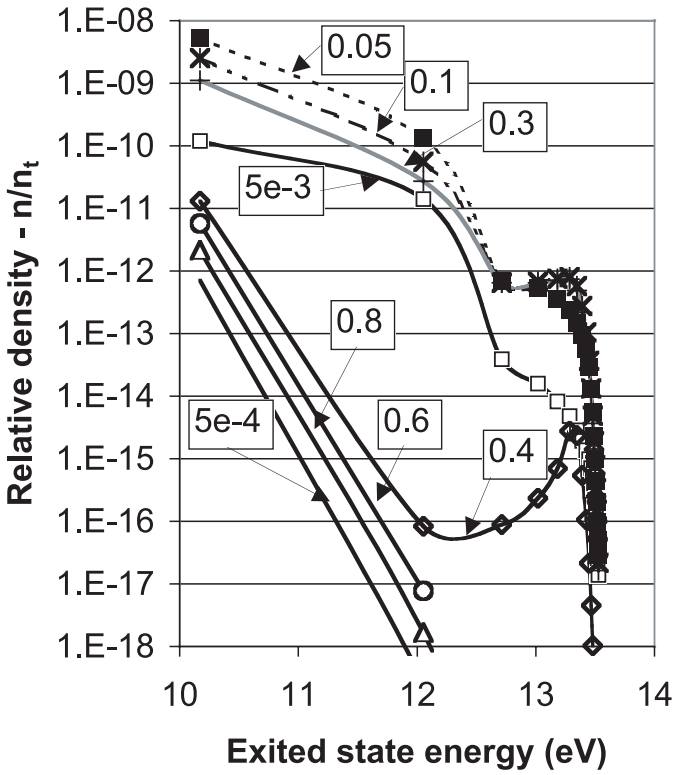

Fig. 4. Electronically atomic H distribution functions versus internal energy for different phase-values $t' = t/T_{cycle}$ in microwave pulsed H_2 discharges ($P = 1$ torr, $MWP_{inp} = 10$ W, $T_{cycle} = 30$ μs, $Duty = 30\%$).

The time evolution of the distribution function of electronically excited states of atomic hydrogen presents a more intriguing trend (see Fig. 4). During the pulse, the concentrations of atomic levels with principal quantum number $n = 2.3$ increase up to $t' = 0.05$ and then decrease, while the concentrations of levels with $n > 3$ carry on increasing up to $t' = 0.1$. They then present a stationary behaviour in the range $0.1 < t' < 0.3$. During the post-discharge phase, the concentrations of $n > 6$ levels decay less rapidly than $n = 2{-}6$ levels, as a result of lower quenching rates. It should be however noted that the population of the $n = 2$ state (in particular the $2s$ hydrogen level) despite their strong quenching rates still keeps non-negligible values during the power-off phase of the cycle. As an example, for $t' = 0.4$ the molar fraction of $n = 2$ level (energy level $\varepsilon^* = 10.2$ eV) is 10^{-11}. It induces a source of electrons at 10.2 eV through second kind collision between cold electrons and excited atomic states, i.e. through the process

$$e(\varepsilon \approx 0) + \mathrm{H}(n = 2, \varepsilon^* = 10.2 \text{ eV}) = e(\varepsilon \approx 10.2) + \mathrm{H}(n = 1, \varepsilon^* = 0). \quad (17)$$

The electron *beam* resulting from this source becomes more pronounced at $t' = 0.35$ and appears as a hump in EEDF at an electron energy of 10.2 eV. Elastic collisions then redistribute this beam until 5 eV for higher t'. Note that the strong effect of second kind collisions in shaping

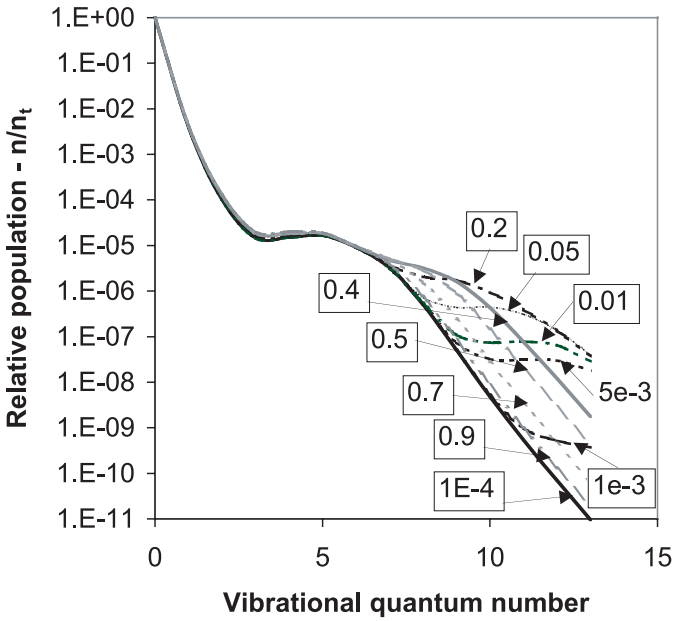

Fig. 5. Molecular hydrogen vibrational distribution for different phase-values $t' = t/T_{cycle}$ in microwave pulsed H_2 discharges ($P = 1$ torr, $MWP_{inp} = 10$ W, $T_{cycle} = 30$ μs, $Duty = 30\%$).

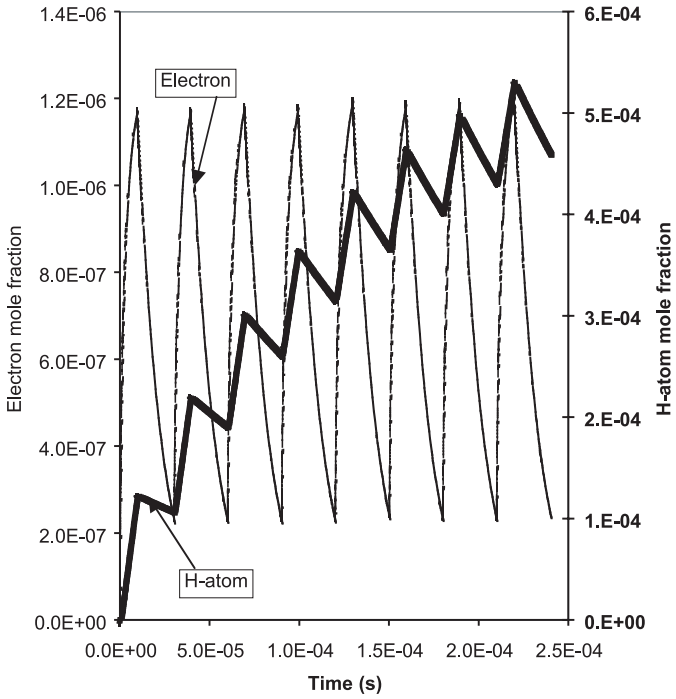

Fig. 6. Time evolution of electron and H-atom molar fractions during different pulse periods ($P = 1$ torr, $MWP_{inp} = 10$ W, $T_{cycle} = 30$ μs, $Duty = 30\%$).

the EEDF is due to the cooling of EEDF through elastic and inelastic collisions.

On the other hand the EEDF's corresponding to the quasistationary part of the power-on fraction of the cycle, i.e. t' in the range 0.05−0.3, do not depend on the presence of electronically excited states because the effect of superelastic collisions is masked by the action of the electric field which provides much stronger heating source for the EEDF. We remind in fact that second kind collisions produce structures on EEDF when the average electron energy is small enough. Interesting in this context is also the EEDF at $t' = 0.33$ and $t' = 0.35$; the effect of second kind collisions due to a multitude of molecular and atomic electronically excited states during the decay of the electric field is very noticeable.

Let us consider now the trend of vibrational distribution function (VDF) during a full cycle. This is shown in Figure 5 for different values of the parameter t'. We see that the VDF is practically frozen for vibrational levels $v < 8$ and shows a large modulation for $v > 8$. The first three levels are mainly produced by the energy excitation processes (Eq. (4)), while levels 4−7 are populated by the stepwise process (Eq. (5)).

Vibration-translation deactivating collisions (Eq. (8)) have too small rates to affect the concentration of levels with the vibrational quantum number in the range 1−7. On the contrary the modulation of the portion of vibrational distribution with $v > 7$ is due to the huge increase of V-T rates with the vibrational quantum number. The increase of VDF for $v > 7$ for t' in the range 10^{-4}−0.2 is therefore the result of continuous pumping of these levels by E-V processes. Then for higher values of t', i.e. for post-discharge phase, the decay of the vibrational distribution function due to V-T deactivating rates takes place.

Let us now consider the time evolution of electron density and neutral atomic species during a large number of cycles. We see in Figure 6 that the electron density reaches a permanent regime in less than 10 periods. The permanent regime is however characterized by a large modulation during each cycle. On the other hand the H-atom concentration reaches a permanent regime only after 50 periods. Figure 7 shows the time-variation of negative ion concentrations. These ions are formed by electron-impact on vibrationally excited molecules, i.e. through the process (DA).

The negative ion concentration is linked to the electron density behaviour showing however a slight increase as a function of the number of cycles. Note that the molar fraction of negative ions is two order of magnitude lower than the corresponding one for electrons, a result in agreement with those of previous modeling investigations [9–11].

Let us now consider an other situation characterized by the same input power (10 W), pressure, and duty cycle (30%), but with a different period (3 ms) compared to the previous case. The results corresponding to this situation are reported in Figures 8 and 9. Figure 8 reports the molar fraction of electrons and H atoms for different cycles and for a total discharge duration of 80 μs (about 27 cycles). The results obtained in this situation are qualitatively similar to those of the previous case which is shown in Figure 6. The difference between the two cases mainly consists in the time delay in achieving a given level of H-atom density when the pulse period is decreased from

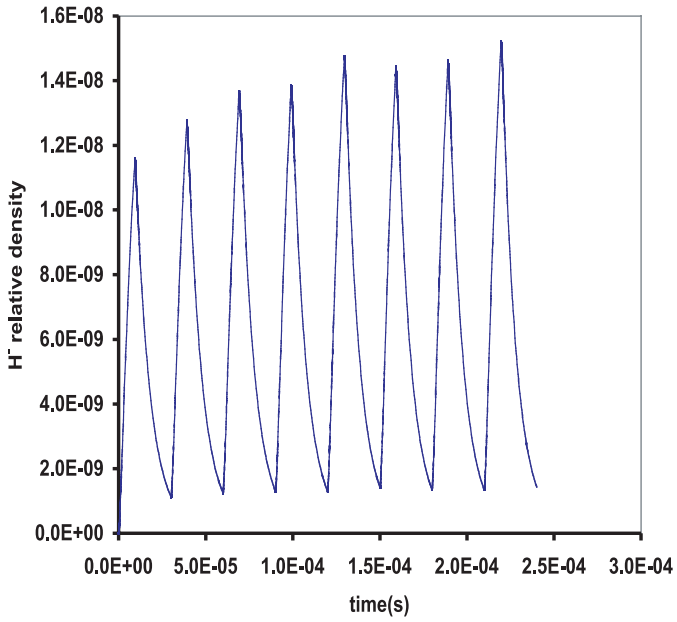

Fig. 7. Time evolution of negative ion (H^-) molar fraction during different pulse periods ($P = 1$ torr, $MWP_{inp} = 10$ W, $T_{cycle} = 30$ μs, $Duty = 30\%$).

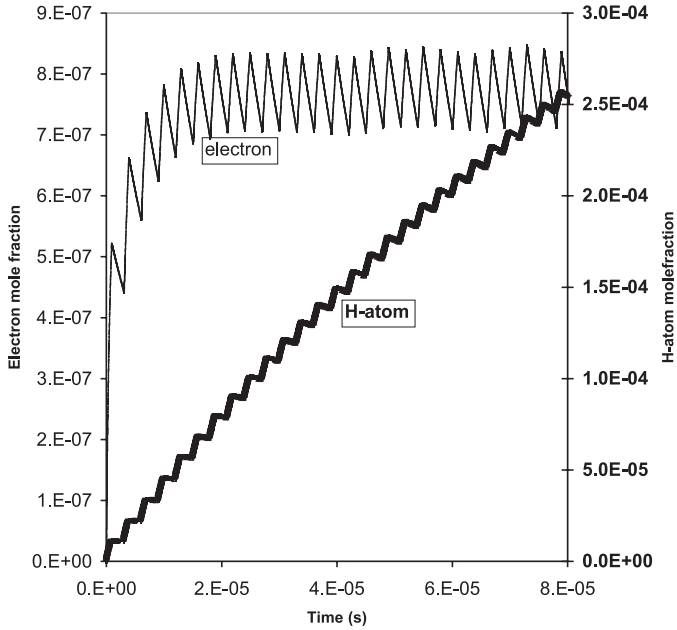

Fig. 8. Time evolution of electron and H-atom molar fractions during different pulse periods ($P = 1$ torr, $MWP_{inp} = 10$ W, $T_{cycle} = 3$ μs, $Duty = 30\%$).

30 to 3 μs. In particular, the molar fractions of electrons and atoms at 80 μs can be recovered in Figure 6 after approximately 3 cycles. On the other hand, we can see from Figure 9 that the population distributions of electronically atomic excited states obtained for periods of 3 μs and 30 μs are similar (Fig. 4). Note however that the relaxation of excited state atomic distribution is lower for the 3 μs case. This causes higher concentrations of excited levels for shorter period. As an example the concentration

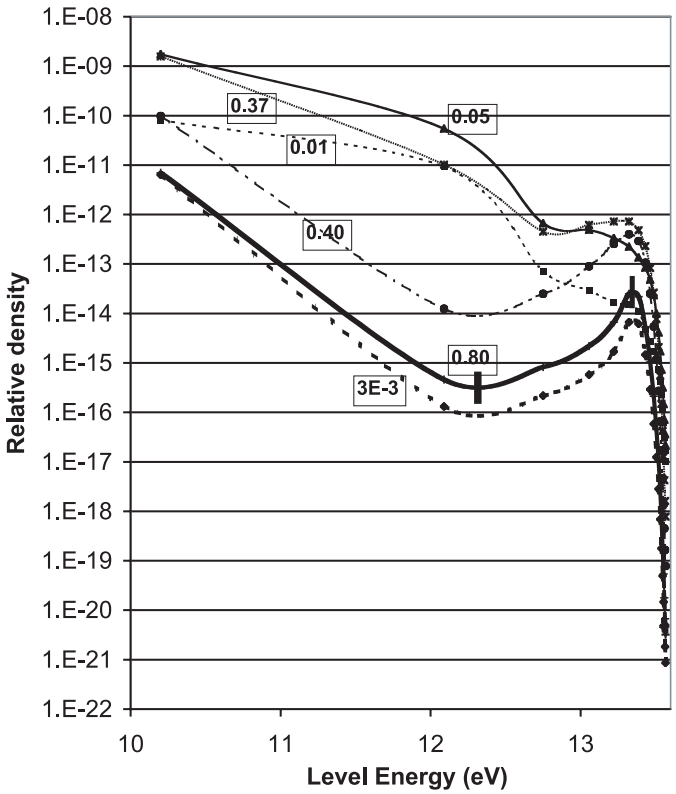

Fig. 9. Electronically excited atomic H distribution functions versus internal energy for different phase-values $t' = t/T_{cycle}$ in microwave pulsed H_2 discharges ($P = 1$ torr, $MWP_{inp} = 10$ W, $T_{cycle} = 3$ μs, $Duty = 30\%$).

of $n = 2$ level (10.2 eV) is one order of magnitude higher for a 3 μs cycle period as compared with the 30 μs case. We would therefore a priori expect a higher influence of superelastic collisions on EEDF. This is however, not the case as may be observed from the comparison of Figures 6 and 10 that show that the EEDF obtained for a 3 μs period is much less structured than that corresponding to 30 μs. This result may be well understood when considering that elastic collisions have no sufficient time to cool the intermediate energy, 5−15 eV, part of EEDF. As a result, although the superelastic collision frequency is high, the high energy electron produced by these collisions are masked by the hot electrons produced during the discharge phase and still remaining in the post-discharge. The time evolution of EEDF is in any case similar to that one found for 30 μs. The higher average energy of electrons smooth out the plateau of Figure 2.

Let us finally discuss the third case similar to the previous one but with much lower pressure (10 mtorr). Typical relaxation times at 10 mtorr (300 K) for the different energy zones of EEDF become two orders of magnitude higher than the corresponding values of the previous cases. Therefore the characteristic times become of the order of 10^2 μs for elastic collisions, 3×10^2 μs for rotational processes and of the order of 10^3 ns for inelastic processes. The characteristic times of elastic and rotational collisions are therefore larger than the considered cycle period.

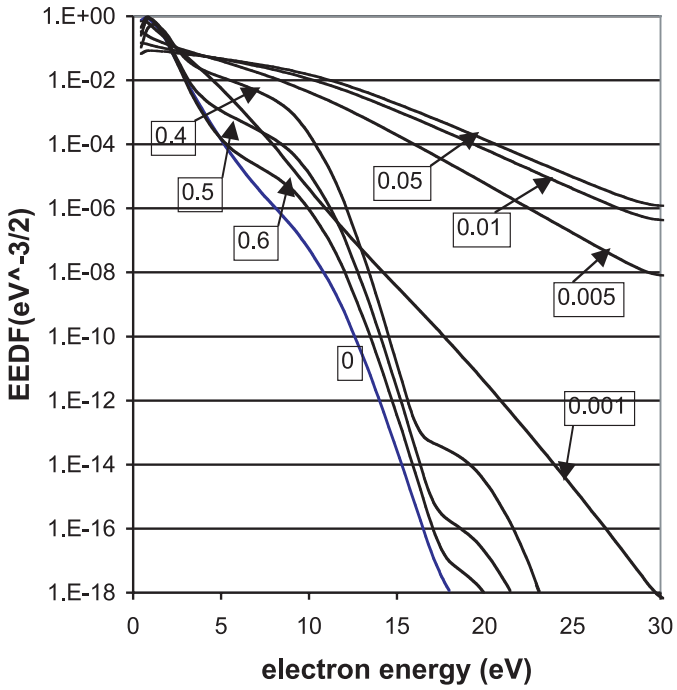

Fig. 10. Electron energy distributions functions versus energy for different phase-values $t' = t/T_{cycle}$ in microwave pulsed H_2 discharges ($P = 1$ torr, $MWP_{inp} = 10$ W, $T_{cycle} = 3$ μs, $Duty = 30\%$).

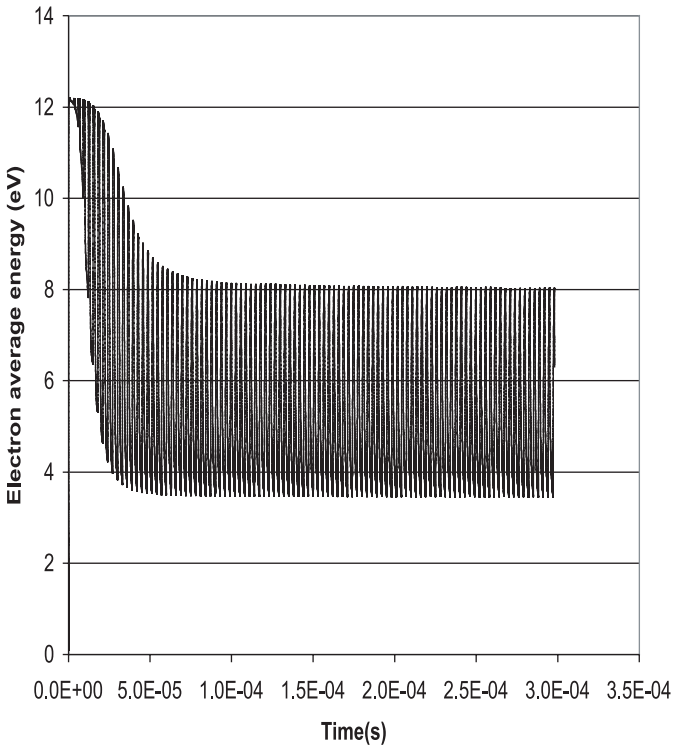

Fig. 11. Time-evolution of the electron average energy in microwave pulsed H_2 discharges ($P = 10$ mtorr, $MWP_{inp} = 10$ W, $T_{cycle} = 3$ μs, $Duty = 30\%$).

We should consequently expect a lower relaxation of all distributions. On the other hand we can expect large E/N values and corresponding increase of the excitation of all distributions.

This point is well evidenced in Figure 11 where we have reported the electron average energy which presents an oscillatory behavior and reaches a permanent periodic regime after approximately 10 cycles. In this periodic regime the average energy oscillates between approximately 8 and 4 eV generating a strong excitation of electronically excited atomic (Fig. 12) and molecular (Fig. 13) states, as well as of strong production of atoms (Fig. 14). For all species we obtain a large increase the concentrations of electronically excited state as compared with the previous cases. For example, electronically excited atomic molar fractions reported in Figure 12 are of the same order of magnitude as the corresponding values of Figure 4 during the power-on fraction of the cycle, and more than two orders of magnitude higher in the post-discharge phase. Similar effects are found for the molar fractions of electronically excited molecular species. However, the large increase of excited state concentrations does not create structures in EEDF (see Fig. 15), since the large values of characteristic times compared with the cycle period prevents the cooling of electrons, thus hiding the effect of electronically excited states in affecting the EEDF. This point is well evidenced in Figure 15 that shows the time evolution of EEDF for this case. We can see that, due to the low pressure, the first part of the distribution ($0 < \varepsilon < 11$ eV) is practically frozen during the cycle, being responsible of the large electron average energies reported in Figure 11.

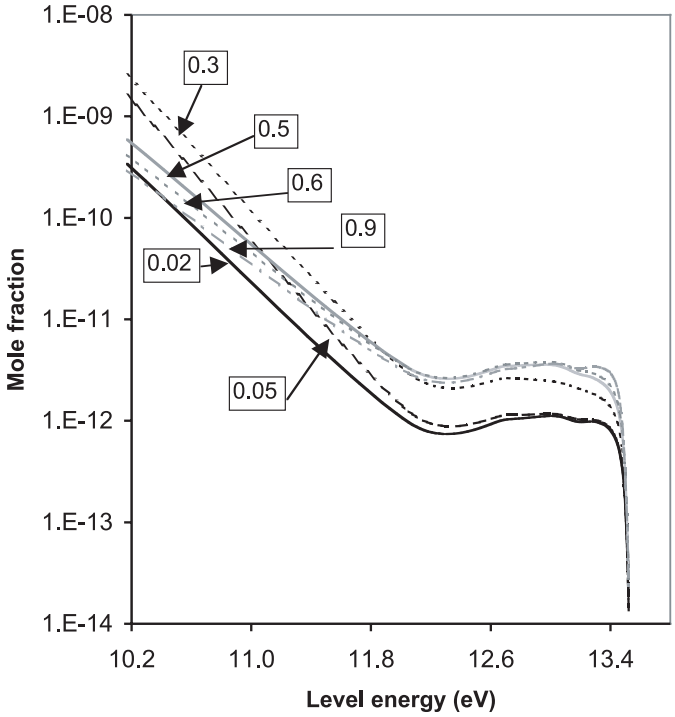

Fig. 12. Electronically atomic H distribution functions versus internal energy for different phase-values $t' = t/T_{cycle}$ in microwave pulsed H_2 discharges ($P = 10$ mtorr, $MWP_{inp} = 10$ W, $T_{cycle} = 3$ μs, $Duty = 30\%$).

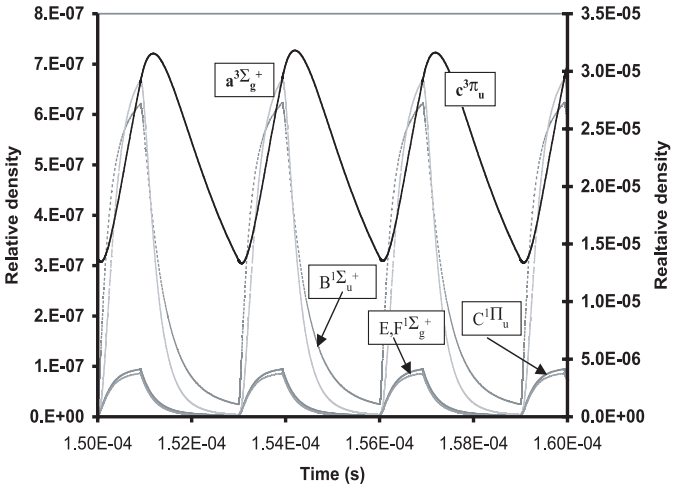

Fig. 13. Time evolution of selected molecular H_2 excited states during different periods (P = 10 mtorr, MWP_{inp} = 10 W, $T_{cycle} = 3$ μs, $Duty = 30\%$).

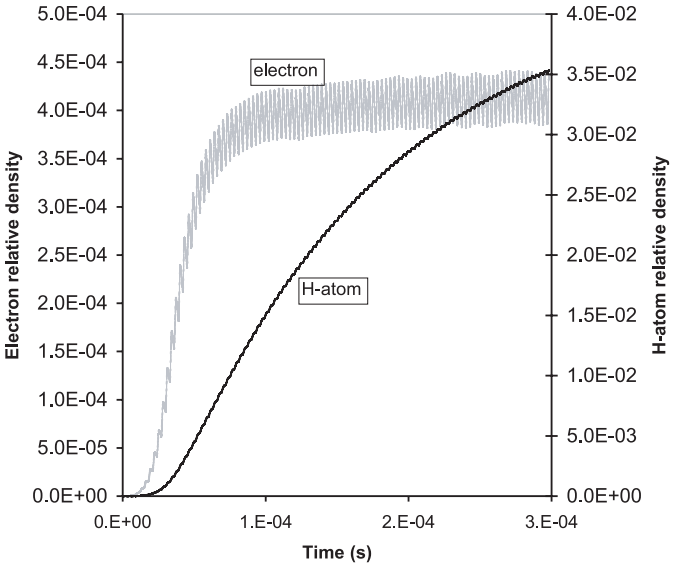

Fig. 14. Time evolution of electron and H-atom molar fractions during different pulse periods ($P = 10$ mtorr, $MWP_{inp} = 10$ W, $T_{cycle} = 3$ μs, $Duty = 30\%$).

The tail of the EEDF is modulated by high-energy threshold inelastic collisions, with characteristic times lower than the cycle period.

Note also that at this low pressure the effect of the power modulation on the excited states populations may differ significantly depending on the considered excited states. The H($n = 2$) excited state population achieves indeed a quasi-periodic dynamics very rapidly (see Fig. 12). This is not the case of the $n > 2$ states, the populations of which do not reach the quasi-periodic regime even after more than 100 periods. The population of these states keep on increasing even during the power-off fraction of the cycle. This is due to the fact that electron average energy and density are still high enough during this phase,

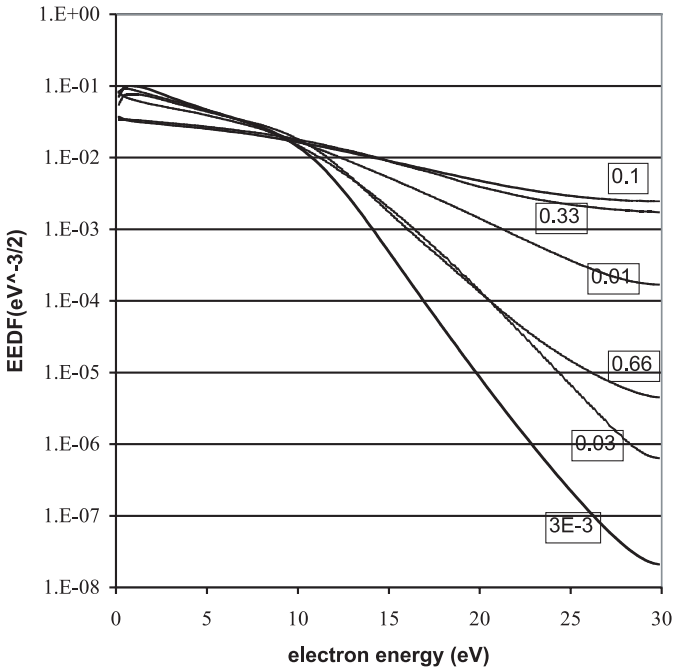

Fig. 15. Electron energy distributions functions versus energy for different phase-values $t' = t/T_{cycle}$ in microwave pulsed H_2 discharges (P = 10 mtorr, MWP_{inp} = 10 W, T_{cycle} = 3 μs, $Duty = 30\%$).

i.e. $\langle \varepsilon_e \rangle > 4$ eV, to induce a significant production rate of these states.

4 Conclusions

In the present paper we have reported the time evolution of non-equilibrium distributions of atomic and molecular species and of free electrons for pulsed microwave discharges. Different case studies have been discussed with the aim of clarifying the temporal behaviour of the different distributions. The main result of this investigation is the strong coupling of EEDF with the distribution functions of electronically atomic and molecular species. This coupling is well evidenced at 1 torr by the appearance of structures in EEDF for conditions characterized by a period of 30 μs and a duty cycle of 30%. On the other hand at low pressure (10 mtorr) and for a period of 3 μs and a duty cycle of 30% and for the same nominal power input (10 W) the structures created by the second kind collisions disappear despite the increase of the concentrations of excited states. In this case we assist indeed to a strong increase of the average electron energy which hides the role of second kind collisions in affecting EEDF.

It should be interesting, as a conclusion, to discuss the possible experimental validation of the present results. Time dependent OES (optical emission spectroscopy) can be used to monitor the distribution functions of electronically excited states for the different conditions. Second derivative Langmuir probes can be effectively used to measure EEDF in a wide range of energy even though the

effect of superelastic collisions seems to be too small for an effective detection. Dedicated experiments, guided by the present theoretical results, can be in any case used to completely understand the kinetics occurring under non equilibrium plasma conditions.

This work has been partially supported by ASI (I/R/055/02).

References

1. K. Hassouni, X. Duten, A. Rousseau, A. Gicquel, J. Electrochem. Soc. **150**(5), C311 (2003)
2. C. Gorse, M. Capitelli, Phys. Rev. A **46**, 2176 (1992)
3. C. Gorse, M. Capitelli, A. Ricard, J. Chem. Phys. **82**, 1900 (1985)
4. K. Hassouni, M. Capitelli, A. Gicquel, Phys. Rev. E **59**, 3741 (1999)
5. K. Hassouni, A. Gicquel, M. Capitelli, J. Loureiro, Plasma Sources Sci. Technol. **8**, 494 (1999)
6. S.D. Rockvood, Phys. Rev. A **8**, 2348 (1973)
7. G. Colonna, C. Gorse, M. Capitelli, R. Winkler, J. Wilhelm, Chem. Phys. Lett. **213**, 5 (1993)
8. M. Capitelli, C. Gorse, J. Wilhelm, R. Winkler, Nuovo Cim. **70**, 163 (1982)
9. K. Hassouni, M. Capitelli, A. Gicquel, Chem. Phys. Lett. **290**, 502 (1998)
10. C. Gorse, R. Celiberto, M. Cacciatore, A. Laganá, M. Capitelli, Chem. Phys. **161**, 211 (1992); C. Gorse, M. Capitelli, M. Bacal, J. Bretagne, A. Laganá, Chem. Phys. **117**, 177 (1987)
11. J. Amorim, J. Loureiro, D.C. Schram, Chem. Phys. Lett. **346**, 443 (2001)